



Cite this: *Chem. Sci.*, 2022, **13**, 13872

All publication charges for this article have been paid for by the Royal Society of Chemistry

Received 9th August 2022
Accepted 8th November 2022

DOI: 10.1039/d2sc04451j
rsc.li/chemical-science

Taming the stilbene radical anion†

Grégoire Sieg,^a Igor Müller,^a Kilian Weißen,^b and C. Gunnar Werncke  ^a

Radical anions appear as intermediates in a variety of organic reductions and have recently garnered interest for their role as mediators for electron-driven catalysis as well as for organic electron conductor materials. Due to their unstable nature, the isolation of such organic radical anions is usually only possible by using extended aromatic systems, whereas non-aromatic unsaturated hydrocarbons have so far only been observed *in situ*. We herein report the first isolation, structure and spectroscopic characterization of a simple aryl substituted alkene radical anion, namely that of stilbene (1,2-diphenyl ethylene), achieved by encapsulation between two $[\text{K}\{18\text{c}6\}]$ cations. The formation of the radical anion is accompanied by $Z \rightarrow E$ isomerization of the involved double bond, also on a catalytic scale. Employing the linear iron(II) complex $[\text{Fe}(\text{NR}_2)_2]^-$ as a reductant and coordination site also allows for this transformation, *via* formation of an iron(II) bound radical anion. The use of the iron complex now also allows for $Z \rightarrow E$ isomerization of electron richer, simple alkenes bearing either mixed alkyl/aryl or even bis(alkyl) substitution.

Introduction

Organic radicals are known to play key roles in many well-established organic reactions. Radical anions, in particular, appear as intermediates in a variety of organic reductions.^{1–3} They are intrinsically unstable due to their ability to react subsequently in a multitude of reaction pathways, such as dimerization, as exploited in pinacol-type coupling reactions.¹ In recent years, organic radical anions have garnered further importance due to the surge of photoredox catalysis.^{4–6} In this context, radical anions are mediators for bond transformations where the transmitted electron itself is sometimes considered as a catalyst in analogy to proton-catalysed reactions.^{7–9} As such there is a longstanding interest in understanding the behaviour of simple radical anions. Common methods to stabilize or even isolate such species rely on the use of extended aromatic systems or electron withdrawing functional groups, such as carbonyl units, to lower the energy of the involved π^* orbitals as well as to disperse of the radical character over a larger π -system.^{10–14} In this instance respective radical anions play an important role in organic functional materials such as electric conductors, transistors or magnetic devices.^{15–19} Isolable examples of pure carbon-based radical anions are still scarce and concern only aromatic compounds with energetically accessible

π^* -orbitals, most prominently alkali metal anthracenes and naphthalenes. In contrast, radical anions of alkene based compounds were so far only observed *in situ*,^{20–23} but are of fundamental interest for nearly a century.²⁴ Of those, the stilbene radical anion $[\text{S}]^{.-}$ (S = stilbene/1,2-diphenylethylene) has been a particular subject of EPR²⁵ and electronic absorption spectroscopic^{26–28} as well as cyclovoltammetric²⁹ analyses. Thereby, the radical anion could only be generated *in situ*, either *via* (electro)chemical reduction,^{25,30,31} photolysis³² or/and radiolysis.³³ It also showed that Z -stilbene is subject to $Z \rightarrow E$ isomerisation, as was extensively examined by Szwarc and others.^{25,30,34–36} Kinetic studies indicated that the isomerisation does not occur *via* the initially formed stilbene radical anion ($Z-[\text{S}]^{.-}$), but the dianion ($Z-[\text{S}]^{2.-}$). The latter stems from reversible disproportionation of $[\text{S}]^{.-}$ (into $[\text{S}]^{2.-}$ and $[\text{S}]^0$), and is thought to isomerise more rapidly than the radical anion $Z-[\text{S}]^{.-}$.^{36–40} Despite these early reports of electron induced alkene $Z \rightarrow E$ isomerisation a use for selective formation of *E*-alkenes from pure *Z*-alkenes or *n* *E/Z*-mixtures, which are often observed in the construction of $\text{C}=\text{C}$ double bonds (*e.g.* by the Wittig reaction, McMurry coupling or alkene metathesis),^{3,41–45} is surprisingly lacking. In part the absence can be explained by the rather harsh reductive conditions, which would be incompatible with functional groups such as halides. With the increasing use of strongly reducing photoredox catalysts such isomerisation reactions might become nonetheless useful. Furthermore, the electrocatalytic $Z \rightarrow E$ isomerisation can pose an alternative for alkene based photoswitches, in resemblance to a recent report of electrocatalytic shifting of the photostationary equilibrium of azobenzene derivatives *via* their radical anions.⁴⁶

Herein we report on the isolation, structure and spectroscopic characterization of the stilbene radical anion, achieved by its encapsulation between two $[\text{K}\{18\text{c}6\}]^+$ cations. The radical

^a Fachbereich Chemie, Philipps-Universität Marburg, Hans-Meerwein-Straße 4, 35037 Marburg, Germany. E-mail: gunnar.werncke@chemie.uni-marburg.de

^b Institut für Chemie, Humboldt-Universität zu Berlin, Brook-Taylor-Str. 2, 12489 Berlin, Germany

† Electronic supplementary information (ESI) available: General, synthetic, analytical and catalytic details, EPR-, ^{57}Fe -Mössbauer-, UV/Vis-, IR-spectra, crystallographic details. CCDC 2214046, 2178651, 2178649 and 2178650. For ESI and crystallographic data in CIF or other electronic format see DOI: <https://doi.org/10.1039/d2sc04451j>



anion readily undergoes reversible electron transfer with excess of *Z*-stilbene, for which accordingly catalytic *Z* \rightarrow *E* isomerisation is observed. Using the linear iron(*i*) silylamide $[\text{Fe}(\text{NR}_2)_2]^-$ the catalytic *Z* \rightarrow *E* isomerisation can conceptionally be extended to 1,2-alkyl/aryl and -dialkyl alkenes, not achievable by the “free” stilbene radical anion. Mechanistic insights point to involvement of an iron(*ii*) bound alkene radical anion.

Results and discussion

Isolation of the stilbene radical anion

Z-Stilbene was reacted with 18-crown-6 and KC_8 in Et_2O in the presence of $[\text{K}\{18\text{c}6\}][\text{Fe}(\text{NR}_2)_3]^{47}$ ($\text{R} = \text{SiMe}_3$). This resulted in an immediate colour change from light yellow to dark red. Storage of the pentane layered reaction solution at -40°C yielded $[(\text{K}\{18\text{c}6\})_2(\text{E-stilbene})][\text{Fe}(\text{NR}_2)_3]$ (**1**) in 61% yield (Scheme 1). The use of $[\text{K}\{18\text{c}6\}][\text{Fe}(\text{NR}_2)_3]$ is of essence as in the absence of the additional $[\text{K}\{18\text{c}6\}]$ cation no reduction of stilbene was observed, while the trisamide serves as a reductively stable non-coordinating anion. Similar observations were already made during the isolation of a phenyl substituted pyridine radical anion.⁴⁸ The $[\text{K}\{18\text{c}6\}]$ cation is equally important moiety as the use of crypt.222 as potassium masking agent resulted in undefined decomposition. **1** is stable at room temperature under inert conditions for several hours in solution and for months in solid state at -35°C . Attempts for the isolation of a *Z*-conformer of **1** were not successful, in agreement with the observed rapid isomerisation to the thermodynamically more stable *E*-conformer.^{25,30,34–36} X-Ray diffraction analysis on suitable crystals revealed the formed *E*-stilbene unit being encapsulated between two $[\text{K}\{18\text{c}6\}]$ cations (Fig. 1 left). The potassium atoms are situated above and below the central alkene unit.

They are pulled slightly out of the plane defined by oxygen atoms of the 18c6 ring, which is indicative of an anionic charge localized on the double bond. Due to an intrinsic, persistent crystallographic problem, unchanged upon variation of the crystallisation conditions, the whole stilbene unit is disordered lengthwise over two positions (1 : 1). Accordingly, this prohibits so far an in-depths evaluation of the structural metrics. For example both crystallographic parts exhibit highly different C–C bonds (1.35 Å and 1.41 Å), which are thus only in part elongated in comparison with the free stilbene (1.34 Å).⁴⁹

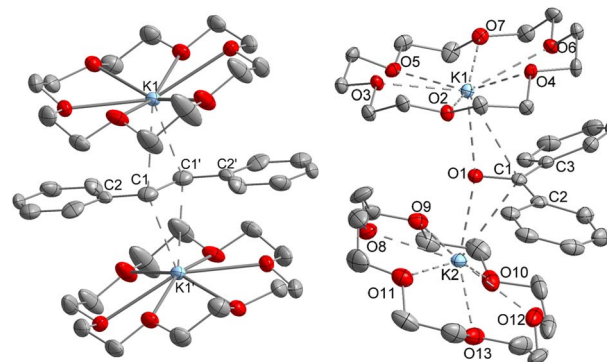
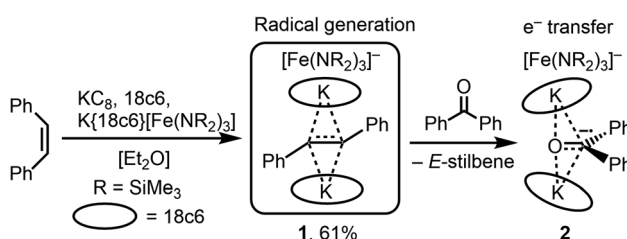


Fig. 1 Molecular structure of **1** (left) and **2** (right) excluding the $[\text{Fe}(\text{N}(\text{SiMe}_3)_2)_3]^-$ counter anions. Hydrogen atoms are omitted for clarity. Selected bond lengths (Å) and angles (°): (1) C1–C1' 1.415(5) [1.350(7)], C1–C2 1.389(7) [1.488(7)], C2–C1–C1' 127.6(4) [125.7(4)]. Bond metrics of the second disordered part are given in square brackets. (2) O1–C1 1.299(2), C1–C2 1.452(2), C1–C3 1.473(2), O1–K1 2.724(1), O1–K2 2.701(1), C1–K1 3.172(1), C1–K2 3.134(2), C2–C1–C3 123.3(1), O1–C1–C2 119.1(1), O1–C1–C3 117.5(1).

To support the notion of a stilbene radical anion, **1** was examined by X-band EPR spectroscopy in toluene. At 8 K the toluene glass of **1** exhibited a hyperfine structured singlet ($g = 2.004088$, Fig. 2), which is in general agreement with the presence of an organic radical anion. The hyperfine structure was however insufficiently resolved to allow for extraction of any coupling constants. The hyperfine structure further lost upon increasing the temperature to 100 K ($g = 2.002396$, Fig. S15†). Here, the observation of an unresolved singlet of the *trans*-stilbene radical anion in frozen solutions at around 100 K is in agreement with respective reports in the literature.^{29,50} Measuring the sample at 298 K also gave a only singlet ($g = 2.002123$, Fig. S14†), which is at odds with reported well resolved EPR spectra of *in situ* formed stilbene radical anions, that show coupling to all hydrogen atoms.^{25,35,51} We attribute the absence of a hyperfine structure for the radical anion in **1** at ambient conditions to persistent ion pairing with the $\text{K}\{18\text{c}6\}$ units, as well as the high-spin iron(*ii*) trisamide counter ion likely also contribute to line broadening *via* spin–spin interactions. Attempts for the measurement of **1** in THF to reduce the ion pairing effect led to its rapid degradation under these dilute



Scheme 1 Synthesis of the bis(cation) stabilized stilbene radical anion **1** and formation of the ketyl complex **2**.

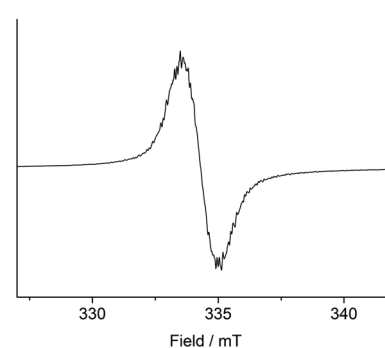
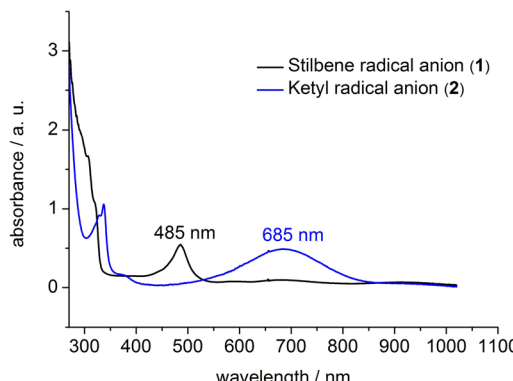


Fig. 2 X-band EPR measurement of **1** in frozen toluene solution (9.368604 GHz) collected at 8 K. $S = \frac{1}{2}$, $g = 2.004088$.



Fig. 3 UV-Vis spectrum of **1** and **2** in THF at 300 K.

conditions. According to its paramagnetic character, the proton NMR spectrum of **1** showed no features beyond the signals attributed to the $[\text{K}\{18\text{c}6\}]$ moieties around 3.47 ppm as well as the $[\text{Fe}(\text{NR}_2)_3]^-$ anion at -2.54 ppm (Fig. S1†). UV-Vis spectroscopic examination of **1** in solution (Fig. 3) revealed a single absorption band at 485 nm which is in good agreement with *in situ* generated $\text{Na}^+(\text{E-stilbene})^\cdot-$ in THF (494 nm).³⁹ The radical anionic nature of **1** was substantiated further chemically as it (incompletely) reduces $[\text{Co}^{\text{II}}(\text{NR}_2)_2]$ to the linear cobalt(*i*) complex $[\text{Co}^{\text{I}}(\text{NR}_2)_2]^-$ (Fig. S8†) whose reduction potential ($E_{\text{red}} = -1.45$ V vs. Fc/Fc^+) is less than of the stilbene ($E_{1/2}$ (*Z*-stilbene) = -2.67 V; $E_{1/2}$ (*E*-stilbene) = -2.70 V vs. Fc/Fc^+).^{29,50,52}

Further, if **1** is subjected to benzophenone ($E_{1/2} = -2.13$ V vs. Fc/Fc^+) the formation of the intensely blue coloured $[(\text{K}\{18\text{c}6\})_2(\text{Ph}_2\text{CO})]_2[\text{Fe}(\text{NR}_2)_3]$ (**2**) is observed (Scheme 1), with a characteristic absorption band at 685 nm belonging to the $\pi \rightarrow \pi^*$ transition of the ketyl radical anion.¹⁴ **2** can also be independently obtained by reducing Ph_2CO with KC_8 in the presence of 18-crown-6 and $[\text{K}\{18\text{c}6\}][\text{Fe}(\text{NR}_2)_2]$. In analogy to **1**, the ketyl radical anion in **2** is sandwiched between the $[\text{K}\{18\text{c}6\}]$ cations (Fig. 1 right). These are tilted towards each other by approximately 42.5° to account for the non-planarity of the diarylketyl unit. The C–O bond length of the ketyl unit in **2** amounts to $1.299(2)$ Å, which is typical for ketyl radical anions and due to a reduced C=O bond order by population of the antibonding π^* orbital^{52,53} (free benzophenone: $1.23(1)$ Å).⁵⁴ Interestingly, besides interactions with the ketyl oxygen ($\text{K1/2-O1} = 2.724(1)$ Å/2.701(1) Å), the potassium cations also exhibit close contacts to the ketyl carbon ($\text{K1/2-C1} = 3.172(1)/3.134(2)$ Å), thus overall coordinating in an asymmetric side-on fashion to the C=O unit. It contrasts the typical end-on coordination of alkali metal ketyl or fluorenyl salts in solid state^{14,55} and is likely due to the repulsion of the opposing crown-ethers. Attempts to acquire radical anions of a more electron rich 1,2-alkyl/aryl-substituted ethylene (β -methyl styrene) or even a 1,2-dialkyl ethylene (3-hexene) were not successful.

Behaviour of the radical anion **1** towards ethylene derivatives

The unequivocal isolation of the cation stabilized stilbene radical anion **1** now offered the opportunity to study with

regards to other alkenes. Quenching **1** with D_2O yielded purely *E*-stilbene, showing that the encapsulated radical anion is not subject to substantial redox disproportionation into stilbene and its dianion as commonly observed during *in situ* studies of stilbene radical anions.^{36–40} Consequently, it implicates that the stilbene radical anion in **1** is responsible for the observed *Z* \rightarrow *E* isomerisation, opposed to the isomerisation mechanism *via* its dianion proposed by Szwarc and others.^{36–40} As such we further wanted to gain insights if **1** can be used for the isomerisation of additional stilbene *via* electron transfer. When **1** was treated with an equimolar amount of *E*-stilbene in THF-d_8 no signs of the added stilbene was perceivable by proton NMR spectroscopy at room temperature or at -80 °C (Fig. S6†). Increasing the amount of *E*-stilbene to 5 equivalents merely hinted to a broad signal centred at the median signal position of *E*-stilbene (7.39 ppm), which became clearly visible using a tenfold excess (Fig. S7†). This speaks to rapid electron transfer between **1** and the added stilbene, that effectuates paramagnetic line broadening. The stilbene addition is accompanied by the appearance of a minor set of signals at around 7.05 ppm as well as at 2.93 ppm, whose amount (approx. 10% with regards to employed **1**) is unaffected by quenching of the reaction mixture with D_2O . We tentatively attributed this to the formation of 1,2,3,4-tetraphenylbutane due to stilbene radical anion dimerization. Given that such a behaviour is absent for **1** itself, it implicates that the presence of additional stilbene leads to minor amounts of free, unstabilised stilbene radical anions, that lack any $[\text{K}\{18\text{c}6\}]$ stabilisation in solution and thus allows for C–C coupling.

To examine the catalytic *Z* \rightarrow *E* isomerisation, *Z*-stilbene (Table 1) was treated with a catalytic amount of **1** (4 mol%) in $[\text{D}_8]\text{THF}$. Conversion to *E*-stilbene is observed within 2.5 h (27% *E*-product) after which the reaction stops as perceived from a colour change from deep yellow to colourless. This is likely due to degradation of the stilbene radical anion in the presence of the substrate,^{37,39} as well as its general instability in $[\text{D}_8]\text{THF}$. Given the proposed involvement of the stilbene radical anion as a reductant, we also tested KC_8 as a catalyst which proved to be highly efficient under the same conditions (100% conversion in $[\text{D}_8]\text{THF}$ within 5 minutes). Interestingly, in Et_2O no isomerisation is observed, showing the importance of potassium

Table 1 Catalytic isomerization of *Z* alkenes in $[\text{D}_8]\text{THF}$ (R = SiMe₃)

Catalyst	R ¹	R ²	Cat. (mol%)	Reaction time	Conversion (%)
1	Ph	Ph	4	2 h 30 min	27%
	Ph	Me	5	20 h	0%
	Et	Et	10	7 d	0%
KC_8	Ph	Ph	4	5 min	100%
	Ph	Me	4	2 h	0%
	Et	Et	10	7d	0%
$\text{K}\{18\text{c}6\}$	Ph	Ph	4	45 min	95%
	$[\text{Fe}^{\text{I}}(\text{NR}_2)_2]$	Ph	Me	10	6 h 30 min
		Et	Et	10	7d
$\text{K}\{18\text{c}6\}$	Ph	Ph	10	3 h 45 min	5.4%
	$[\text{Fe}^{\text{I}}(\text{NR}\{\text{Dipp}\})_2]$	Ph	Ph	10	24 h
					12%



cation solvation. Expanding the catalytic isomerisation to a 1,2-alkyl/aryl-substituted (*Z*- β -methyl styrene) or *Z*-1,2-dialkyl ethylene derivative (*Z*-3-hexene) using **1** or KC_8 as catalyst did not result in any transformation at all, which can be explained by the substrates' more electron rich nature.

Iron mediated *Z* \rightarrow *E* isomerisation of alkenes

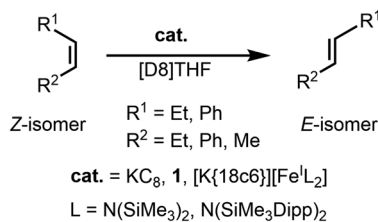
To overcome these shortcomings in terms of *Z* \rightarrow *E* isomerisation of alkylated ethylene derivatives we contemplated on isomerisation of such species in the coordination sphere of a highly reducing metal complex (Scheme 2). For that we chose the iron(i) silylamine $[\text{Fe}^{\text{I}}(\text{NR}_2)_2]^-$ ($E_{\text{red}} = -2.07$ V),⁵⁶ which was already proven for the formation of iron(ii) bound radical anions of ketones and related nitrogen derivatives (imines and aldimines), as well as of alkynes.^{52,57} Further, a remarkable yet slow *Z* \rightarrow *E* isomerisation was observed recently for an ethylene bridged diphosphine (*cis*-1,2-bis(diphosphino)ethylene).⁴⁷ Indeed, using 4 mol% of $[\text{K}\{18\text{c}6\}][\text{Fe}^{\text{I}}(\text{NR}_2)_2]$ *Z*-stilbene is converted to *E*-stilbene by 95% within 45 minutes.

Intriguingly, *Z*- β -methylstyrene as well as even *Z*-3-hexene are also transformed, however needing higher catalyst loadings (10 mol%) and substantially longer reaction times (Fig. 4). The slower reaction can be attributed to the increase of the π^* -orbital energy in case of alkyl substituents.

Mechanistic examination of these catalytic reactions gave pseudo-first order kinetics for these iron mediated transformations, with no signs of an induction phase. To further

substantiate the direct involvement of $[\text{K}\{18\text{c}6\}][\text{Fe}^{\text{I}}(\text{NR}_2)_2]$ we conducted poisoning experiments, to rule out the involvement of *in situ* formed iron nanoparticles. Addition of stoichiometric amounts of 2,2'-bipyridine to the reaction mixture, proven to bind tightly to $[\text{Fe}(\text{NR}_2)_2]^-$,⁵⁸ stopped the reaction. Upon addition of further $[\text{Fe}(\text{NR}_2)_2]^-$ the catalysis resumed (Fig. 4, bottom right). Conversely, the system is unaffected by the addition of an excess of PCy_3 which does not interact with $[\text{Fe}(\text{NR}_2)_2]^-$,⁵⁶ but influences the activity of nanoparticles.^{59,60} To explore the steric effect of the iron(i) catalyst, the same transformations were conducted with the sterically more demanding complex $[\text{K}\{18\text{c}6\}][\text{Fe}^{\text{I}}(\text{NR}\{\text{Dipp}\})_2]$ ⁶¹ (Table 1). While a *Z* to *E* isomerization is still observable for stilbene, the reaction proceeds considerably slower, and is absent in case of the alkylated ethylene derivatives.

Stoichiometric treatment of $[\text{K}\{18\text{c}6\}][\text{Fe}(\text{NR}_2)_2]$ with the substrates in Et_2O resulted in an instantaneous change of colour of the solution from green to reddish brown in case of *Z*-stilbene. Crystallisation from the pentane layered Et_2O filtrate gave the π complex $[\text{K}\{18\text{c}6\}][\text{Fe}(\text{NR}_2)_2(\text{E-stilbene})]$ (**3**) in moderate yields (54%) (Scheme 3). Within **3** the substrate coordinates to iron in a η^2 fashion (Fig. 5, left). The central C–C bond (1.384(5) Å) is elongated in comparison with free stilbene (1.338 Å).⁴⁹ The elongation is in the common range for alkenes bound to a low-valent metal ion,^{62,63} and is usually attributed to $\text{p} \rightarrow \pi^*$ backbonding.^{64–66} The alkene ligand is twisted slightly (15.6(3)°) with regards to the plane defined by the N1,Fe1 and N2 yielding a distorted square planar geometry around the metal. The Fe–N distances amount to approx. 1.99 Å. This is



Scheme 2 Catalytic *Z* to *E* conversion of alkenes with $[\text{Fe}^{\text{I}}]$ as catalyst.

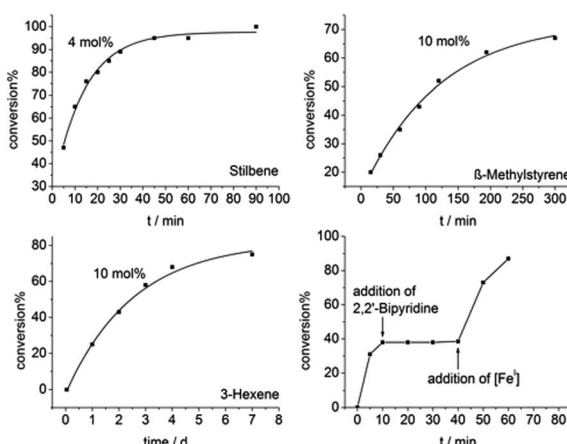
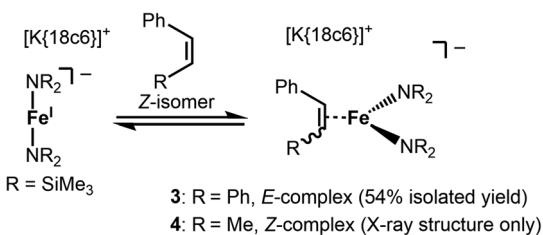


Fig. 4 Catalytic *Z* to *E* conversion for stilbene (top left), β -methylstyrene (top right), 3-hexene (bottom left) using $[\text{Fe}^{\text{I}}]$ as catalyst and poisoning experiment with 2,2'-bipyridine (bottom right).



Scheme 3 Formation of the side-on alkene complexes **3** and **4** in solution.

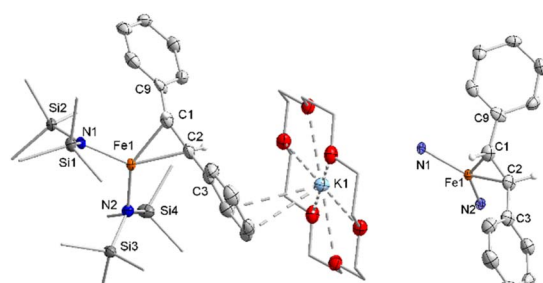


Fig. 5 Molecular structure of **3** in the solid state (left) and depiction of the central iron-alkene unit. Unnecessary H atoms are omitted for clarity. Selected bond lengths (Å) and angles (°): Fe1–N1 1.995(2), Fe1–N2 1.990(2), Fe1–C1 2.109(3), Fe1–C2 2.112(3), C2–C3 1.384(5), N1–Fe1–N2 115.64(10).



larger than in the iron(i) precursor (1.92 \AA)⁵⁶ and comparable to three coordinate iron(ii) halide complexes ($1.95\text{--}1.97\text{ \AA}$)⁶⁷ as well as the previously reported related π -alkyne iron complexes $[\text{Fe}(\text{NR}_2)_2(\eta^2\text{-RCCR})]$ ($1.97\text{--}2.00\text{ \AA}$).⁶⁸ To substantiate the oxidation state of iron in **3** zero-field ^{57}Fe -Mössbauer spectroscopy was employed (Fig. 6).

The spectrum of **3** at 13 K shows a doublet signal for the main species with an isomer shift of $\delta = 0.53\text{ mm s}^{-1}$ and a quadrupole splitting of $\Delta Q = 1.44\text{ mm s}^{-1}$. The isomer shift corresponds very well with low coordinate iron(ii) complexes ($[\text{Fe}(\text{NR}_2)_3]^-$: $\delta = 0.59\text{ mm s}^{-1}$, $\Delta Q = 0.60\text{ mm s}^{-1}$; $[\text{Fe}(\text{NR}_2)_2\text{I}]^-$: $\delta = 0.63\text{ mm s}^{-1}$, $\Delta Q = 0.60\text{ mm s}^{-1}$; $[\text{Fe}(\text{NR}_2)_2\text{OCPH}_2^{(\cdot)}]^{(-)}$: $\delta = 0.62\text{ mm s}^{-1}$, $\Delta Q = 1.20/1.83\text{ mm s}^{-1}$).^{52,56,69} The Mössbauer data implicates the formulation of **3** as an iron(ii) bound alkene radical anion. Such a description is indeed plausible in view of DFT and CASSCF studies on the interaction of alkynes with $[\text{Fe}(\text{NR}_2)_2]^-$ (ref. 57) and a T-shaped iron(i) complex⁷⁰ which were best described as metal(ii) bound alkyne radical anions.

X-band EPR spectroscopic measurements at 100 K performed on **3** in THF gave no pronounced features. The absence of any signal rules out the presence of an iron(i) ion ($S = 3/2$) and supports the notion of a non-Kramer's iron(ii) ion ($S = 2$) coupled to an organic radical.

^1H -NMR spectroscopic examination of isolated **3** gave a resonance for the SiMe_3 -groups at -6.01 ppm (Fig. S3†). This signal position exhibits a slight high-field shift in comparison to either trigonal π -alkyne iron or three-coordinate iron(ii) hexamethyldisilazanides (-1.88 to -4.05 ppm).^{52,57,67} Additional resonances at 92.7 ppm , 91.2 ppm and -25.3 ppm are attributed to aromatic substrate protons. Importantly, dissolution of pristine **3** gave rise to a signal belonging to the initially employed $[\text{Fe}(\text{NR}_2)_2]^-$ as well as *E*-stilbene. This implicated a dissociation equilibrium of **3** in solution, corroborated by independent measurement of a 1:1 mixture of *Z*-stilbene and $[\text{K}\{18\text{c}6\}][\text{Fe}(\text{NR}_2)_2]$. No evidence of the initial formation of the *Z*-alkene adduct $[\text{Fe}(\text{NR}_2)_2(\text{Z-stilbene})]$ by proton NMR spectroscopy was found, hinting to rapid bond isomerisation.

For the treatment of *Z*- β -methyl styrene with $[\text{K}\{18\text{c}6\}][\text{Fe}(\text{NR}_2)_2]$ the colour change upon substrate addition was less pronounced. Attempts for the isolation of the adduct yielded only few crystals of the π -alkene complex **4** (see Fig. S33†) which were obtained with inseparable amounts of unreacted, crystalline $[\text{K}\{18\text{c}6\}][\text{Fe}(\text{NR}_2)_2]$. The structure of the anion in **4** is

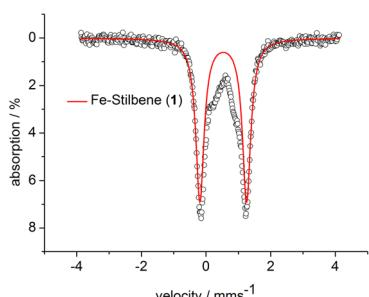
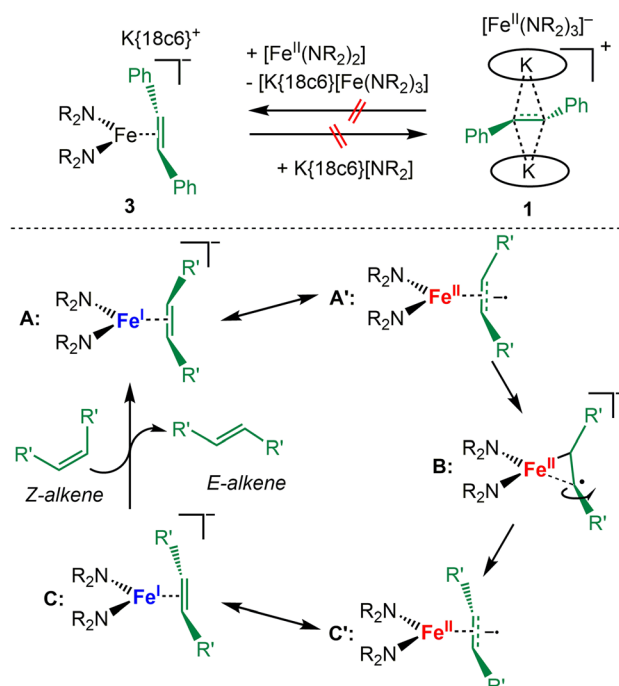


Fig. 6 Zero-field ^{57}Fe -Mössbauer spectrum of **3** at 13 K. $\delta = 0.53\text{ mm s}^{-1}$, $\Delta Q = 1.44\text{ mm s}^{-1}$.

similar to the one found for **3** with a slightly shorter C2–C3 distance ($1.416(3)\text{ \AA}$) but exhibits otherwise comparable bond metrics. Proton NMR spectroscopic examination of a 1:1 mixture of the iron(i) precursor with equimolar amounts of *Z*- β -methyl styrene in [D8]THF resulted in the observation of a minor signal at -5.36 ppm belonging to the SiMe_3 groups of **4** (Fig. S4†), with major amount of the iron(i) precursor and free stilbene. The latter is found only as the *E*-isomer. For the even more electron rich *Z*-3-hexene no signs of a π -complex are observed in solution, or upon crystallisation attempts. Together with the observations made for **3**, it implicates an equilibrium between the free substrate as well as the iron(i) precursors and the respective adduct complex in solution, which is shifted to the former upon employing more electron rich substrates.

To probe the possible dissociation of **3** into the neutral iron(ii) amide $[\text{Fe}(\text{NR}_2)_2]$ and the free radical anion it was treated with KNR_2 and 18c6 which however did not lead to the replacement of the alkene radical anion with the hexamethyldisilazanide and formation of **1** (Scheme 4, top). Inversely, the reaction of **1** with an excess of $[\text{Fe}^{\text{II}}(\text{NR}_2)_2]$ did also not yield **3** – which could occur either by direct coordination the radical anion to $[\text{Fe}^{\text{II}}(\text{NR}_2)_2]$ or *via* its outer-sphere reduction as seen for $[\text{Co}^{\text{II}}(\text{NR}_2)_2]$ under subsequent alkene coordination. As such the isomerisation of the ethylene derivative in **3** likely proceeds in the coordination sphere of the iron ion, and substrate dissociation occurs not as a free radical anion but as a neutral species. We thus propose for iron a catalytic cycle that starts with *Z*-alkene binding to the linear iron(i) silylamine (Scheme 4,



Scheme 4 Top: Attempted conversion of **3** and **1** into each other. Bottom: Proposed mechanism for the *Z* to *E* isomerization of alkenes with $[\text{Fe}^{\text{I}}]$ as catalyst. Coordination of the *Z*-alkene to the metal ion as π - (A) or radical anion (A') complex; B: rotation along the C–C bond; C/C' *E*-alkene complex.



bottom). The π -complex **A** (as in complex **4**) can also be described as an iron(II) bound *Z*-alkene radical anion (**A'**). Subsequently, weakening of one Fe-C bond would allow for rotation along the C-C bond (**B**). Such an asymmetric substrate binding was found as a stable and energetically feasible state in case of related alkyne chromium complexes.⁵⁷ This yields in an *E*-alkene complex (*C/C'*, as complex **3**). Finally, the formed *E*-alkene is replaced by the next *Z*-alkene.

Conclusions

In conclusion, we presented the isolation and characterisation of a long time elusive simple alkene radical anion, namely the *E*-stilbene radical anion. This otherwise fleeting species is stabilized by encapsulation between two [K{18c6}] units. Similarly, coordination of stilbene to the highly reducing iron(I) complex $[\text{Fe}(\text{NR}_2)_2]^-$ ($\text{R} = \text{SiMe}_3$) leads to a situation best described as a metal(II) bound alkene radical anion. In both cases, the radical anion formation can be used for catalytic *Z* \rightarrow *E* isomerisation of C=C double bonds. The stilbene radical anion can only isomerize stilbene itself, whereas the transformation can be conceptionally extended to harder to reduce 1,2-alkyl/aryl and dialkyl ethylene using the iron(I) complex K{18c6} $[\text{Fe}(\text{NR}_2)_2]$. This reductively induced *Z* \rightarrow *E* isomerisation of alkenes might pose a complementary approach for the photo switching of alkenes, similar to the previously mentioned report on the electrocatalytic isomerisation of azobenzenes.⁴⁶

Data availability

All experimental procedures, spectral data, and computational data are included in the ESI.† NMR/EPR/IR/Mössbauer raw data is so far only available upon request to C. G. W.

Author contributions

G. S. and I. M. carried out the synthetic work and analytical characterization, including the crystallographic studies. K. W. performed the ^{57}Fe Mössbauer analysis. G. S. and C. G. W. wrote the manuscript.

Conflicts of interest

There are no conflicts to declare.

Acknowledgements

We thank Prof. Dr Christian Limberg (HU Berlin) for access to the Mössbauer spectrometer, as well as Dr Andreas Stoy, Prof. Dr Crispin Lichtenberg, Amanda O. Basilio, and Prof Dr Kallof Ray for the acquisition of EPR-spectroscopic data. The Philipps-University and the Deutsche Forschungsgemeinschaft (DFG) is acknowledged for funding (grants WE 5627/4-1 and WE 5627/4-2).

Notes and references

- 1 T. Wirth, *Angew. Chem., Int. Ed.*, 1996, **35**, 61–63.
- 2 M. L. Di Vona and V. Rosnati, *J. Org. Chem.*, 1991, **56**, 4269–4273.
- 3 M. Ephritikhine, *Chem. Commun.*, 1998, 2549–2554.
- 4 M. Zhang, W. D. Rouch and R. D. McCully, *Eur. J. Org. Chem.*, 2012, 6187–6196.
- 5 S. Okamoto, K. Kojiyama, H. Tsujioka and A. Sudo, *Chem. Commun.*, 2016, **52**, 11339–11342.
- 6 S. Okamoto, R. Ariki, H. Tsujioka and A. Sudo, *J. Org. Chem.*, 2017, **82**, 9731–9736.
- 7 A. Studer and D. P. Curran, *Nat. Chem.*, 2014, **6**, 765–773.
- 8 D. W. Borhani and F. D. Greene, *J. Org. Chem.*, 1986, **51**, 1563–1570.
- 9 D. Leifert, C. G. Daniliuc and A. Studer, *Org. Lett.*, 2013, **15**, 6286–6289.
- 10 K. Kato and A. Osuka, *Angew. Chem., Int. Ed.*, 2019, **131**, 9074–9082.
- 11 M. Irwin, R. K. Jenkins, M. S. Denning, T. Krämer, F. Grandjean, G. J. Long, R. Herchel, J. E. McGrady and J. M. Goicoechea, *Inorg. Chem.*, 2010, **49**, 6160–6171.
- 12 M. Irwin, T. Krämer, J. E. McGrady and J. M. Goicoechea, *Inorg. Chem.*, 2011, **50**, 5006–5014.
- 13 M. Irwin, L. R. Doyle, T. Krämer, R. Herchel, J. E. McGrady and J. M. Goicoechea, *Inorg. Chem.*, 2012, **51**, 12301–12312.
- 14 T. A. Scott, B. A. Ooro, D. J. Collins, M. Shatruk, A. Yakovenko, K. R. Dunbar and H.-C. Zhou, *Chem. Commun.*, 2009, 65–67.
- 15 C. S. Sevov, R. E. M. Brooner, E. Chénard, R. S. Assary, J. S. Moore, J. Rodríguez-López and M. S. Sanford, *J. Am. Chem. Soc.*, 2015, **137**, 14465–14472.
- 16 Y. Che, A. Datar, X. Yang, T. Naddo, J. Zhao and L. Zang, *J. Am. Chem. Soc.*, 2007, **129**, 6354–6355.
- 17 X. Zhan, A. Facchetti, S. Barlow, T. J. Marks, M. A. Ratner, M. R. Wasielewski and S. R. Marder, *Adv. Mater.*, 2011, **23**, 268–284.
- 18 H. Iwamura, *Polyhedron*, 2013, **66**, 3–14.
- 19 S. Kumar, Y. Kumar, S. Keshri and P. Mukhopadhyay, *Magnetochemistry*, 2016, **2**, 42.
- 20 G. J. Hoijtink and P. H. Van der Meij, *Z. Phys. Chem.*, 1959, **20**, 1–14.
- 21 M. Szwarc, Application of Spectroscopic and Electrochemical Techniques in Studies of Chemistry of Radical Anions and Dianions, in *Characterization of Solutes in Nonaqueous Solvents*, ed. G. Mamantov, Springer, Boston, MA, 1978.
- 22 J. Matsuda, J. Jagur-Grodzinski and M. Szwarc, *Proc. R. Soc. London, Ser. A*, 1965, **288**, 212–223.
- 23 H. Muto, K. Nunome and K. Matsuura, *J. Am. Chem. Soc.*, 1991, **113**, 1840–1841.
- 24 W. Schlenk and E. Bergmann, *Justus Liebigs Ann. Chem.*, 1928, **463**, 1–97.
- 25 F. Gerson, H. Ohya-Nishiguchi, M. Szwarc and G. Levin, *Chem. Phys. Lett.*, 1977, **52**, 587–589.



26 H. Suzuki, K. Koyano, T. Shida and A. Kira, *Bull. Chem. Soc. Jpn.*, 1982, **55**, 3690–3701.

27 H. Suzuki, K. Ogawa, T. Shida and A. Kira, *Bull. Chem. Soc. Jpn.*, 1983, **56**, 66–74.

28 C. N. R. Rao, V. Kalyanaraman and M. V. George, *Appl. Spectrosc. Rev.*, 1970, **3**, 153–228.

29 O. Abdul-Rahim, A. N. Simonov, J. F. Boas, T. Rüther, D. J. Collins, P. Perlmutter and A. M. Bond, *J. Phys. Chem. B*, 2014, **118**, 3183–3191.

30 K. Nozaki, A. Naito, T.-I. Ho, H. Hatano and S. Okazaki, *Chem. Lett.*, 1989, 511–514.

31 G. F. Wright, *J. Am. Chem. Soc.*, 1939, **61**, 2106–2110.

32 T. Majima, M. Fukui, A. Ishida and S. Takamuku, *J. Phys. Chem.*, 1996, **100**, 8913–8919.

33 J. R. Langan and G. A. Salmon, *J. Chem. Soc., Faraday Trans. 1*, 1982, **78**, 3645.

34 C. S. Johnson and R. Chang, *J. Chem. Phys.*, 1965, **43**, 3183–3192.

35 R. Chang and C. S. Johnson, *J. Chem. Phys.*, 1967, **46**, 2314–2316.

36 S. Sorensen, G. Levin and M. Szwarc, *J. Am. Chem. Soc.*, 1975, **97**, 2341–2345.

37 T. A. Ward, G. Levin and M. Szwarc, *J. Am. Chem. Soc.*, 1975, **97**, 258–261.

38 G. Levin, T. A. Ward and M. Szwarc, *J. Am. Chem. Soc.*, 1974, **96**, 270–272.

39 H. C. Wang, G. Levin and M. Szwarc, *J. Am. Chem. Soc.*, 1977, **99**, 2642–2647.

40 L. R. Dosser, J. B. Pallix, G. H. Atkinson, H. C. Wang, G. Levin and M. Szwarc, *Chem. Phys. Lett.*, 1979, **62**, 555–561.

41 B. E. Maryanoff and A. B. Reitz, *Chem. Rev.*, 1989, **89**, 863–927.

42 B. E. Maryanoff, A. B. Reitz, M. S. Mutter, R. R. Whittle and R. A. Olofson, *J. Am. Chem. Soc.*, 1986, **108**, 7664–7678.

43 W.-Y. Siau, Y. Zhang and Y. Zhao, in *Stereoselective Alkene Synthesis*, ed. J. Wang, Springer Berlin Heidelberg, Berlin, Heidelberg, 2012, vol. 327, pp. 33–58.

44 J. E. McMurry, *Chem. Rev.*, 1989, **89**, 1513–1524.

45 A. Fürstner, *Science*, 2013, **341**, 1229713.

46 A. Goulet-Hanssens, M. Utecht, D. Mutruc, E. Titov, J. Schwarz, L. Grubert, D. Bléger, P. Saalfrank and S. Hecht, *J. Am. Chem. Soc.*, 2017, **139**, 335–341.

47 C. G. Werncke and I. Müller, *Chem. Commun.*, 2020, **56**, 2268–2271.

48 I. Müller and C. G. Werncke, *Chem.-Eur. J.*, 2021, **27**, 4932–4938.

49 A. Hoekstra, P. Meertens and A. Vos, *Acta Crystallogr., Sect. B: Struct. Sci., Cryst. Eng. Mater.*, 1975, **31**, 2813–2817.

50 O. Abdul-Rahim, A. N. Simonov, T. Rüther, J. F. Boas, A. A. J. Torriero, D. J. Collins, P. Perlmutter and A. M. Bond, *Anal. Chem.*, 2013, **85**, 6113–6120.

51 R. Chang and C. S. Johnson, *J. Chem. Phys.*, 1964, **41**, 3272–3274.

52 G. Sieg, Q. Pessemesse, S. Reith, S. Yelin, C. Limberg, D. Munz and C. G. Werncke, *Chem.-Eur. J.*, 2021, **27**, 16760–16767.

53 K. C. MacLeod, I. M. DiMucci, E. P. Zovinka, S. F. McWilliams, B. Q. Mercado, K. M. Lancaster and P. L. Holland, *Organometallics*, 2019, **38**, 4224–4232.

54 E. B. Fleischer, N. Sung and S. Hawkinson, *J. Phys. Chem.*, 1968, **72**, 4311–4312.

55 Z. Hou, A. Fujita, T. Koizumi, H. Yamazaki and Y. Wakatsuki, *Organometallics*, 1999, **18**, 1979–1985.

56 C. G. Werncke, P. C. Bunting, C. Duhayon, J. R. Long, S. Bontemps and S. Sabo-Etienne, *Angew. Chem., Int. Ed.*, 2015, **54**, 245–248.

57 I. Müller, D. Munz and C. G. Werncke, *Inorg. Chem.*, 2020, **59**, 9521–9537.

58 I. Müller, C. Schneider, C. Pietzonka, F. Kraus and C. G. Werncke, *Inorganics*, 2019, **7**, 117.

59 D. Gärtner, S. Sandl and A. Jacobi von Wangenheim, *Catal. Sci. Technol.*, 2020, **10**, 3502–3514.

60 J. F. Sonnenberg and R. H. Morris, *Catal. Sci. Technol.*, 2014, **4**, 3426–3438.

61 C.-Y. Lin, J. C. Fettinger, F. Grandjean, G. J. Long and P. P. Power, *Inorg. Chem.*, 2014, **53**, 9400–9406.

62 Y. Yu, J. M. Smith, C. J. Flaschenriem and P. L. Holland, *Inorg. Chem.*, 2006, **45**, 5742–5751.

63 I. Nieto, F. Ding, R. P. Bontchev, H. Wang and J. M. Smith, *J. Am. Chem. Soc.*, 2008, **130**, 2716–2717.

64 M. Dewar, *Bull. Soc. Chim. Fr.*, 1951, **18**, C78.

65 C. Elschenbroich, *Organometallics*, Wiley-VCH, Weinheim, 3rd edn, 2006.

66 O. Eisenstein and R. Hoffmann, *J. Am. Chem. Soc.*, 1981, **103**, 4308–4320.

67 C. G. Werncke, J. Pfeiffer, I. Müller, L. Vendier, S. Sabo-Etienne and S. Bontemps, *Dalton Trans.*, 2019, **48**, 1757–1765.

68 R. Weller, I. Müller, C. Duhayon, S. Sabo-Etienne, S. Bontemps and C. G. Werncke, *Dalton Trans.*, 2021, **50**, 4890–4903.

69 A. Eichhöfer, Y. Lan, V. Mereacre, T. Bodenstein and F. Weigend, *Inorg. Chem.*, 2014, **53**, 1962–1974.

70 J. C. Ott, H. Wadeohl and L. H. Gade, *Inorg. Chem.*, 2021, **60**, 3927–3938.

